

# Transient Deformation during Triggered Seismicity from the 28 June 1992 $M_w = 7.3$ Landers Earthquake at Long Valley Volcanic Caldera, California

by M. J. S. Johnston, D. P. Hill, A. T. Linde, J. Langbein, and R. Bilham

**Abstract** Continuous records from a borehole strainmeter and a long baseline tiltmeter in the Long Valley caldera provide critical insights into the origin of at least one episode of minor seismicity in volcanic regions triggered by the 28 June 1992,  $M_L$  7.3 Landers, California, earthquake. A strain transient reaching a peak of 0.25 microstrain occurred in the few days following the Landers event and decayed over the next 20 days. A tilt perturbation during the same time reached a peak amplitude of 0.2 microradians. These signals correspond approximately in time to the primary seismic moment release across a 50 km<sup>2</sup> region of the south part of the caldera at depths between 2 and 10 km. Corresponding strain transients in 5-km geodetic lines across the south caldera are not apparent above the 95% confidence limits of about 0.4 microstrain in daily sampled data during this same period. These data rule out models involving single localized inflation sources within the upper crust beneath the caldera, including that responsible for the current rapid inflation of the resurgent dome. They also preclude models involving aseismic slip on single strike-slip or normal faults in the caldera. A single source in the form of a relaxing magma body at a depth of 50 km beneath the caldera can account for the deformation data, but whether the small stress changes are sufficient to drive the triggered seismicity is not clear. An alternate possibility involves distributed deformational sources triggered by the passage of the 10 microstrain peak amplitude surface waves from the earthquake. This distributed deformational source could result either from rupturing of overpressured fluid or gas chambers commonly encountered in volcanic regions or from advective gas overpressure during release of gas bubbles in hydrothermal or magmatic fluids.

## Introduction

Clear examples of regional triggered seismicity following large earthquakes are rare, and clarification of the physical mechanisms involved is difficult to achieve from seismic network data alone. Proposed mechanisms include enhanced fault connectivity (Bodin and Gomberg, 1994), aseismic fault slip triggered by dynamic strain (Anderson *et al.*, 1994; Gomberg and Bodin, 1994), and relaxation of partly crystallized magma bodies (Hill *et al.*, 1993). Fortunately, the 28 June 1992  $M_w$  7.3 Landers earthquake produced unambiguous triggered seismicity in numerous regions of the western United States (Hill *et al.*, 1993), mostly where there is evidence of recent volcanic activity. At one of these locations, the Long Valley caldera in eastern California (Fig. 1), triggered seismicity and deformation were recorded simultaneously for the first time. These records provide hints about the physical mechanism(s) responsible for the triggered seismicity.

Our continuous deformation measurement systems consist of a borehole dilational strainmeter capable of reliably

recording strain during large ground acceleration (Sacks *et al.*, 1971) and a long-base tiltmeter (Beavan, 1991). Also, approximately daily measurements are made of 4 to 8 km geodetic lines across the caldera with a two-color geodimeter. Line lengths from site CASA (Fig. 1) are measured to a precision of about 0.2 microstrain (Langbein *et al.*, 1989). The borehole strainmeter POPA is installed at a depth of 162 m and provides strain data at periods from minutes to months at a measurement precision of between 0.001 microstrain and 0.01 microstrain. Earth tidal strain and atmospheric pressure loading strains are routinely removed from the data using linear least-squares techniques (Johnston *et al.*, 1986). Data are transmitted to the USGS in Menlo Park, California, through the GOES satellite once every 10 min (Silverman *et al.*, 1989) and are recorded on site with digital and analog recorders. The tiltmeter LBT has orthogonal legs with lengths of 423 and 449 m in directions of east–west and north–south, respectively. Vertical ground displacement of the end bench marks in relation to the fluid reference surface

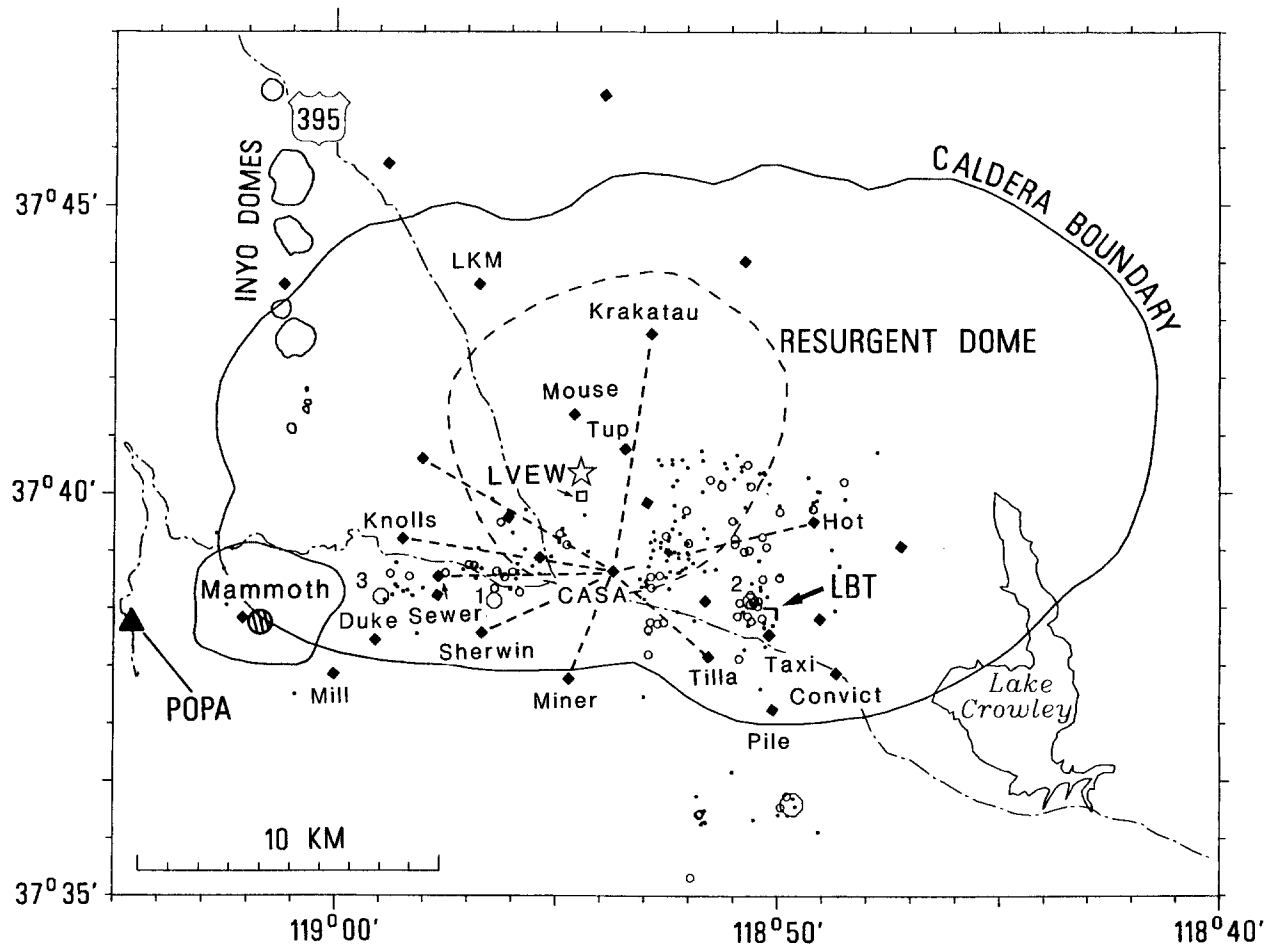


Figure 1. Location of borehole strainmeter POPA, longbase tiltmeter LBT, deep borehole LVEW (open square), two-color geodetic benchmarks (diamonds), and triggered seismicity from 28 June to 20 August 1992 in the Long Valley Caldera. Location of the deformation source generating  $>3$  microstrain/yr in this region since 1989 is  $\approx 7$  km beneath the LVEW deep borehole and is shown as an open star.

is measured with a Michelson interferometer. The tilt measurement precision from minutes to months is between 0.005 and 0.05 microradians. These data are also transmitted through the GOES satellite.

### Observations

Figure 2 is a plot of cumulative seismicity and strain from 10 June to 20 August 1992. North-south and east-west tilt are plotted until 20 July, when the thermal compensation failed. The Landers earthquake occurred at 1157 UT on 28 June 1992 (Kanamori *et al.*, 1992) and was located in the Mojave desert some 430 km south-southeast of Long Valley caldera. Strain and tilt data shown in Figure 2 have the atmospheric pressure loading signal removed and are superimposed on the same data with earth tidal strains removed. The onsite digital record at 100 Hz sampling was unfortunately not in operation during the earthquake. Close inspection of the onsite analog record indicates the onset of the

compressive strain transient apparently occurs during the passage of the Landers earthquake surface waves through the region. The surface waves at the POPA strainmeter have a peak amplitude of 10 microstrain. The strain transient reaches a maximum amplitude of about 0.25 microstrain after 5 days and decays over the next few weeks. The strain, seismicity, and tilt signals during the first 10 days can be fit with equations of the form  $A[1 - \exp(-at)]$  and the rise times of these exponential-like increases are all about 2 days (Hill *et al.*, 1995).

The triggered seismicity during the 3-day period immediately following the Landers earthquake occurred primarily in a 5- by 15-km area within the southwest quadrant of the caldera (Fig. 1). The induced events occurred throughout the same depth range (2 to 10 km) and with the same lateral extent as persistent activity before the Landers earthquake (Hill *et al.*, 1995). This "south moat" region of the caldera has been active since 1980. The Landers earthquake apparently stimulated the processes responsible for the ongoing seismicity patterns. The earthquakes had magnitudes

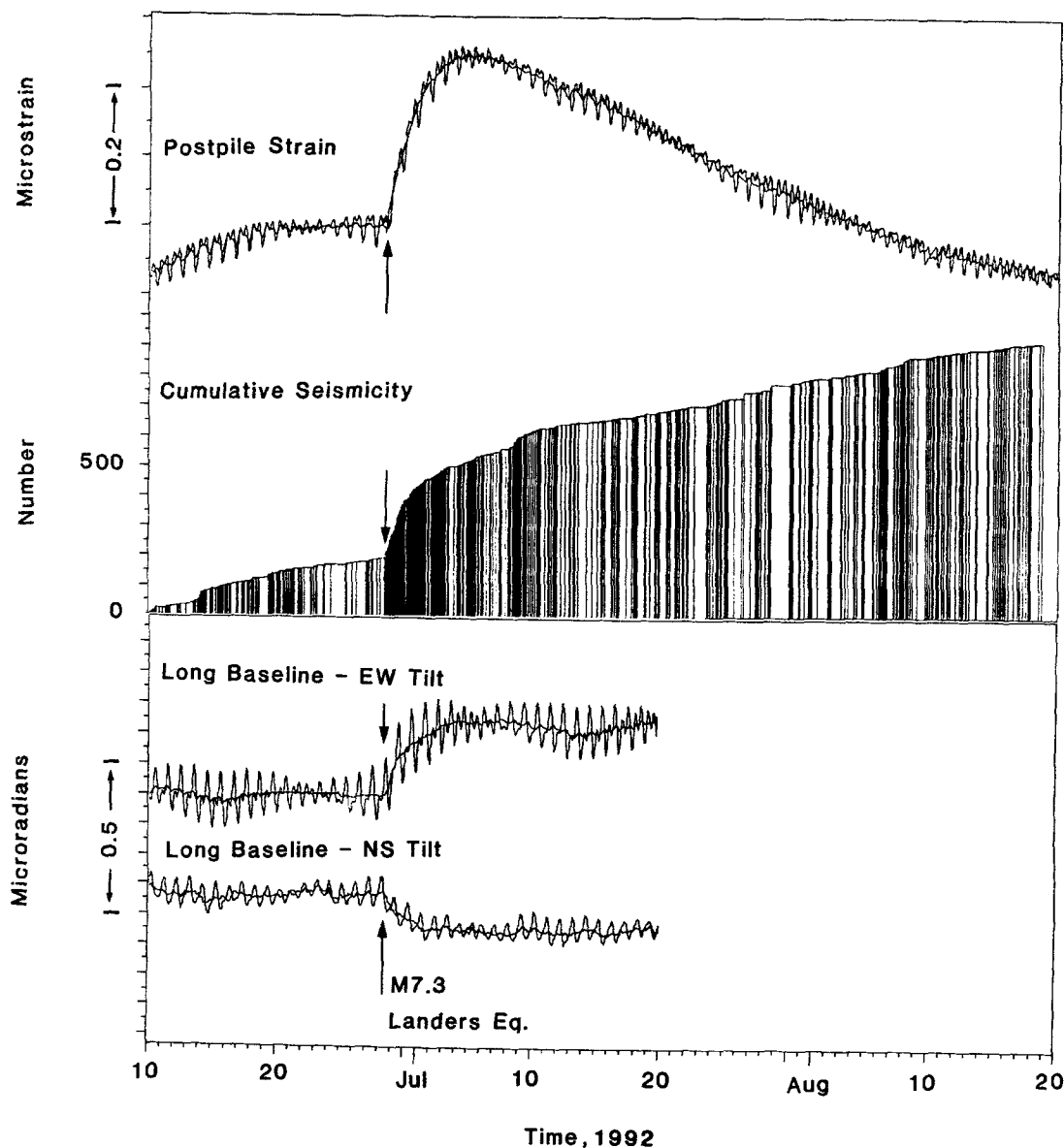


Figure 2. Plot of strain (upper plot), cumulative seismicity (second plot), and tilt (third and fourth plots) from 10 June to 20 Aug 1992. The occurrence time of the Landers earthquake is shown with an arrow on each record.

up to 3.4. The three largest events were  $M$  2.8 at 1230 UT on 28 June about 3 min after the Landers earthquake,  $M$  2.9 at 0304 UT in 29 June and  $M$  3.4 at 0758 UT on 29 June. The first of the larger events was at a depth of 9 km beneath Sherwin (number 1 on Fig. 1), the second event was at a depth of 8.5 km beneath the long base tiltmeter LBT (number 2 on Fig. 1), and the third was at a depth of 7.5 km just south of Knolls (number 3 on Fig. 1). In general, there are no clear spatial migration patterns in the seismicity. The total moment release within the caldera of about  $10^{22}$  dyne-cm (equivalent to about one  $M$  4 earthquake) is 10 to 100 times too small to explain the observed tilts and strains.

A tilt transient was recorded on the longbase fluid tiltmeter (LBT) at the Mammoth Lakes airport during this same period. Figure 2 (lower two plots) shows these data with and

without the solid earth tides. The onset is most clear on the east-west component and has a comparable rise-time constant ( $\approx 2$  days) to that in the strain and seismicity data. The onset in the north-south tilt data is not at all clear. The tilt reached a peak amplitude of 0.2 microradian down to the east after about 5 days and then decayed over the next week.

No significant changes in displacement were detected at the time of Landers in measurements of two-color geodimeter baselines within the caldera. Figure 3 shows strain (i.e., displacement change/line length) time histories for four representative lines over the south moat area (Knolls, Sherwin, Miner, and Tilla; Fig. 1). The standard deviation in these data is 0.15 microstrain. Assuming that the strain changes are isotropic, we can determine the maximum changes in average volumetric strain ( $\Delta$ ) and maximum shear strain  $\gamma_{\max}$

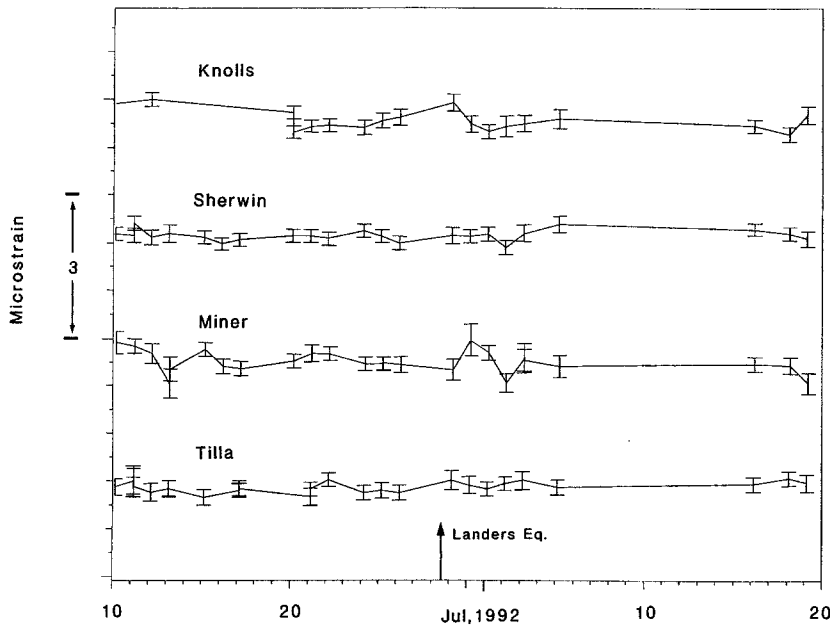


Figure 3. Strain time histories from four two-color geodetic lines (Knolls (7.04 km), Sherwin (4.9 km), Miner (4 km) and Tilla (4.2 km)) over the south moat area during the critical time period from 10 June to 20 July. The occurrence time of the Landers earthquake is shown with an arrow.

at the ground surface within the caldera during this time that could not be detected in the two-color data. The value of  $\Delta$  is determined from

$$\Delta \approx \frac{(1 - 2\nu)}{(1 - \nu)} (e_1 + e_2),$$

where  $\nu$  is Poisson's ratio (usually about 0.25 to 0.3) and  $e_1$  and  $e_2$  are the principal strains. Shear strain  $\gamma_{\max}$  is determined from

$$\gamma_{\max} = (e_1 - e_2)$$

At the 95% confidence limits ( $\approx \pm 2\sigma$ ), changes in  $\Delta$  would need to be greater than  $\approx 0.4$  microstrain to be detectable, while changes in  $\gamma_{\max}$  would need to be greater than  $\approx 0.3$  microstrain (Langbein *et al.*, 1989). Thus, the physical process responsible for the strain and tilt changes detected by the volumetric strainmeter and the tiltmeter did not produce calderawide dilatation and shear strain greater than about 0.4 microstrain.

Other large earthquakes of similar magnitude and at similar distances, with similar surface-wave amplitudes and comparable coda duration, did not produce such a triggered response in seismicity, strain, or tilt in Long Valley caldera. These events include the 18 October 1989  $M$  7.2 Loma Prieta earthquake ( $\delta = 268$  km) and the 25 April 1992  $M$  7.1 Petrolia earthquake ( $\delta = 723$  km). Figure 4 shows simultaneous dilational strain, cumulative seismicity, and tilt (similar to that shown in Fig. 2) during the time of the Loma Prieta earthquake. The Petrolia and Loma Prieta events triggered seismicity at the Geysers geothermal area in northern California (Davis, 1993) and the Coso geothermal field in Owens Valley (Roquemore and Simila, 1994), in addition

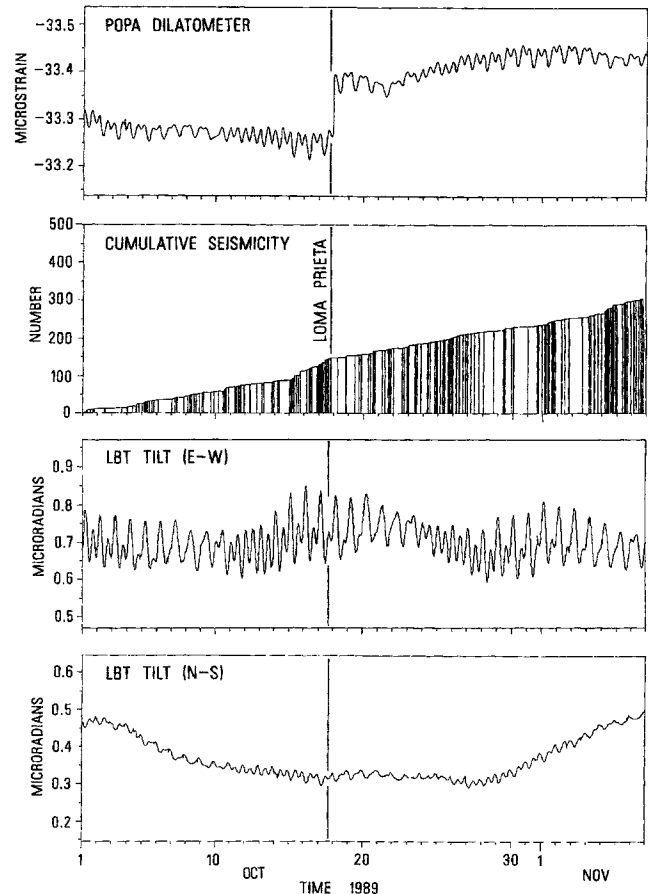


Figure 4. Plot of dilational strain at POPA (upper plot), cumulative seismicity (second plot), and tilt (third and fourth plots) from 1 October to 6 November 1989. The occurrence time of the Loma Prieta earthquake is shown with a vertical line on each record.

to the triggered activity following the Landers earthquake (Hill *et al.*, 1993). Unfortunately, no deformation data are available in these areas to investigate the mechanics of the triggering source. Triggered seismicity, strain, or tilt changes also were not observed at the Long Valley caldera following closer, smaller events for which (1) the peak strainwave amplitudes were about half those of the Landers earthquake, (2) the signal content was richer in high-frequency energy (i.e., shorter wavelength), and (3) the coda durations were 5 to 6 times shorter. These events include 20 June 1987  $M$  6.4 Chalfant earthquake ( $\delta = 49$  km) (Figure 5) and the 17 May 1993  $M$  6.0 Eureka Valley earthquake ( $\delta = 120$  km).

Thus, the dynamic strains during the Landers earthquake were the highest this region has experienced during the past 10 yr but only by about a factor of 2. The duration of shaking and frequency content of the straingram was comparable to that produced by Loma Prieta and Petrolia earthquakes. The dynamic strain field generated by the Landers earthquake apparently exceeded some nonlinear threshold in the state of the crust beneath the Long Valley caldera that was not quite reached by waves from other earthquakes. This threshold may have been lowered by the continuing rapid deformation of the caldera, and thus made a triggered response more likely during Landers than during the Loma Prieta, Petrolia, or other earthquakes.

### Discussion

It is clear that triggered deformation and seismicity generated by the Landers earthquake in the Long Valley Caldera resulted from physical processes within the crust beneath the caldera. What can we infer about these processes with the records from these few instruments? An obvious candidate for a source process is the current source of inflation beneath the resurgent dome. Since mid-1989, the caldera has undergone systematic uplift and horizontal extension of about 3 microstrain/yr that is largely consistent with a simple point inflation source at a depth of about 7 km under the resurgent dome (Langbein *et al.*, 1993). The location of the source is shown in Figure 1 as an open star near the "Mouse" endpoint. The high dynamic strains during the Landers earthquake might have somehow accelerated inflation at this location.

We have used forward-modeling searches through this region and have been unable to find a simple, single pressure source at this location beneath the caldera that produces the observed strain and tilt data but does not generate displacements on the two-color lines of more than a few millimeters. The various source types tried include spherical pressure sources (Mogi, 1958) and ellipsoidal pressure sources (Davis, 1986). We have also tried, again without success, to find single inflation sources at other locations within the seismogenic zone in the caldera and beneath Mammoth mountain. We have extended this search to include possible aseismic slip on known single normal and strike-slip faults using simple elastic dislocation models (Okada, 1992) of faults in

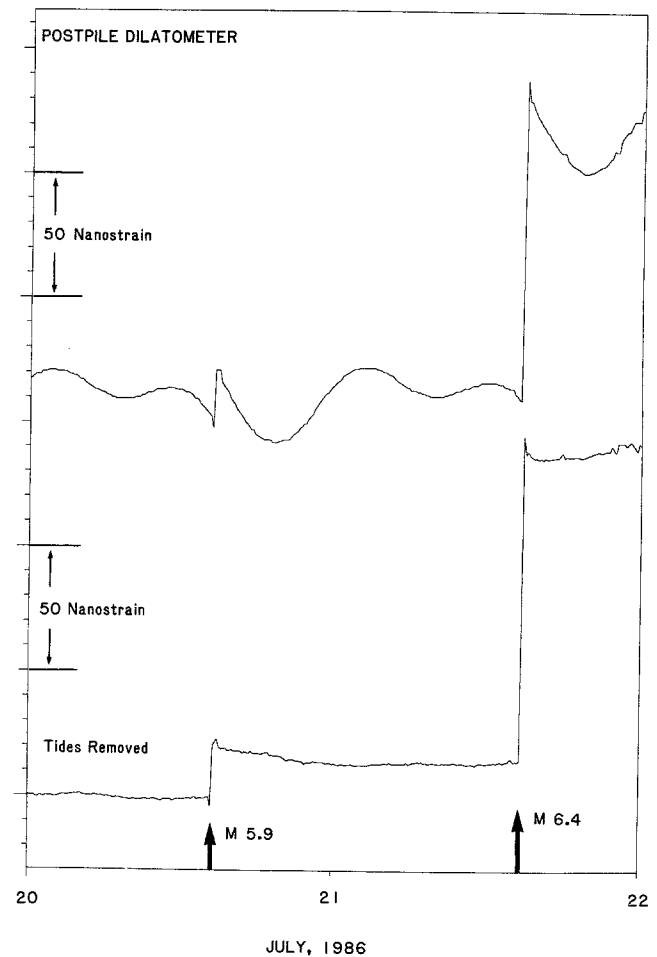


Figure 5. Strain time history at the Postpile strainmeter (POPA) during the  $M$  6.4 Chalfant earthquake on 21 July 1986 and its  $M$  5.9 foreshock on 20 July. The upper plot shows the raw data and the lower plot shows the same data with earth tides removed.

the region. A large, single source beneath the seismogenic zone representing fluidization of a partially crystallized magma body at a depth of 50 km can satisfy the data (Hill *et al.*, 1995). In this case, the body is deep enough to produce displacements across the caldera less than the measurement errors of the two-color geodetic system. The moment release ( $\approx 10^{25}$  dyne-cm) is large enough to give the correct amplitude and sense of strain at POPA if the source is almost beneath the tiltmeter, and the correct tilt amplitude and direction can be achieved if the location beneath the tiltmeter is such that a tilt nodal line is just to the east to the tiltmeter site. Thus, this uniquely positioned single source is capable of producing similar tilt and strain time histories at sites 20 km apart. However, the small stress changes from this source advance the stress state in the seismogenic region within the caldera only marginally (by about 0.1 bar) toward Coulomb failure. Whether these stress changes are sufficient to drive the triggered seismicity is not altogether clear. Larger stress generated by deformation sources closer to (or within) the seismogenic volume can drive the triggered seismicity, but

at the cost of appealing to the coincidence of two or more spatially distinct sources evolving with the same source-time function.

A common, distributed deformational source within the seismogenic region thus has considerable appeal as a mechanism for simultaneously driving the triggered seismicity (spanning an area of more than 50 km<sup>2</sup>) and the tilt and strain transients (20-km site separation) all with a common temporal evolution. The form of all these signals indicates an exponential-like increase in each during the first 10 days following the Landers earthquake with a time constant of about 2 days followed (less clearly) by a gradual decay over the next several weeks.

Another important clue may lie in the fact that much of the triggered seismicity occurred in regions of geologically recent (<1 Ma) volcanism (Hill *et al.*, 1993). A common aspect of volcanic or geothermal regions is the presence of regions containing superhydrostatic fluid pressure that result from compression following rapid chemical sealing of fractures and veins (Fournier, 1991). Because quartz solubility dramatically reduces with decreasing pore pressure (Fournier, 1985; Herrington and Wilkinson, 1993), earthquake and/or volcanic activity that opens previously sealed fractures in these regions and lowers the pore pressure will result in rapid deposition of vein minerals. Deposition reseals the cracks and fractures and allows superhydrostatic pore fluid pressures to be reestablished in newly sealed compartments as the tectonic load on the region is increased (Byerlee, 1993). High-temperature laboratory measurements (Moore *et al.*, 1994) indicate that, following fracture, permeability changes of three orders of magnitude occur in only a few days from rapid silica deposition. The seismogenic region in the south moat of the Long Valley caldera and under Mammoth mountain may well contain numerous regions of high pore pressure that have been increasingly loaded as the caldera inflated initially in the 1980s (Langbein, 1989) and more rapidly since 1989 (Langbein *et al.*, 1993). Rupture and interconnection of many of these high-pore-pressure compartments during the passage of large-amplitude surface waves from the Landers earthquake would cause an upward surge in pore fluids that gradually choke off after several days by silica deposition as the initial pore pressure  $P_c$  decreases within the chamber.

For vertical cracks, the pore pressure in the fracture as a function of time and position has the form (Fenoglio *et al.*, 1994)

$$P(z, t) = P_c \operatorname{erfc} \left( \frac{z}{2\sqrt{Dt}} \right), \quad (1)$$

where *erfc* is the complementary error function  $D = \kappa\eta\beta\phi$ , where  $\kappa$  is fracture permeability,  $\eta$  is dynamic viscosity,  $\beta$  is fluid compressibility,  $\phi$  is porosity, and  $z$  is vertical direction. This pore pressure distribution is shown in Figure 6a as a function of  $z/2\sqrt{Dt}$ . To the strainmeter and tiltmeter,

the initial deformation field would result from a combination of that from a deflating pressure source and an inflating propagating crack with a diffusion time constant determined by crack geometry and fracture permeability. A later phase of the deformation field results from diffusive propagation of fluids into the surrounding region. For an observed time constant of 2 days, with dynamic viscosity for brine,  $\eta = 10^{-4}$  Pa·sec, fluid compressibility,  $\beta = 3.6 \times 10^{-10}$  Pa<sup>-1</sup>, porosity,  $\phi = 0.5$ , and fracture permeability,  $\kappa = 10^{-14}$  m<sup>2</sup>, we calculate crack lengths of  $\approx 400$  m. Pressure as a function of time at the end of such a 400-m fracture is shown (dotted line) in Figure 6b. Pressure decrease in the chamber will have a similar time constant but opposite sign. For comparison, we superimpose the observed strain record from POPA on the pressure record in Figure 6b.

The moment release for an opening crack with a length of 400 m is roughly  $M_0 = 6 \times 10^{20}$  dyne-cm, or the equivalent of a  $M$  2.7 earthquake. To produce the observed strain and tilt transients, cracks of this size would have to extend to within 1 km of the surface beneath the POPA and LBT sites. Larger cracks would, of course, generate larger moments and could be deeper. To explain the onset of triggered seismicity, at depths largely between 1 and 10 km, other cracks/pore pressure changes must have occurred throughout the seismogenic crust beneath the caldera. Thus, under this model, we imagine a surge of pore pressure changes throughout the seismogenic crust, all driven by a distribution of failed overpressured zones as a result of the large dynamic waves from Landers.

Because the crack system is not hydrologically isolated from the surrounding region, the diffuse flow outward would be expected to have a much longer time constant than that generated by flow in the crack system. While we have no direct knowledge of the intermediate depth permeability structure, it is likely to be about  $10^{-15}$  m<sup>2</sup> or 1 mDarcy (du Plessis and Roos, 1994), at least an order of magnitude below the permeability of the crack system. Increased pore pressure will trigger earthquakes because, as the pore fluid pressure is increased in the surrounding region, the effective stress is decreased and existing faults are weakened (Bell and Nur, 1978). Seismicity triggered in this manner has been observed to occur under dams, where pressure changes from water level changes of as small as 0.01 MPa (0.1 bar) trigger earthquakes (Simpson and Negmatullaev, 1981). Diffusion of this pressure pulse through the region could explain the longer-term indications of strain and seismicity decay with time.

Pressure pulses with diffusion decay may also result by releasing gas bubbles trapped by surface tension within hydrothermal fluid or magma filled regions during large-amplitude surface-wave shaking. The upward migration of these gas bubbles produces advective gas overpressure, as proposed by Sahagian and Proussevich (1992). As shown in detail by Linde *et al.*, (1994), upward migration over several days could provide pressure increases of MPa/100 m within the chamber for bubble sizes <1 cm and fluid viscosities of

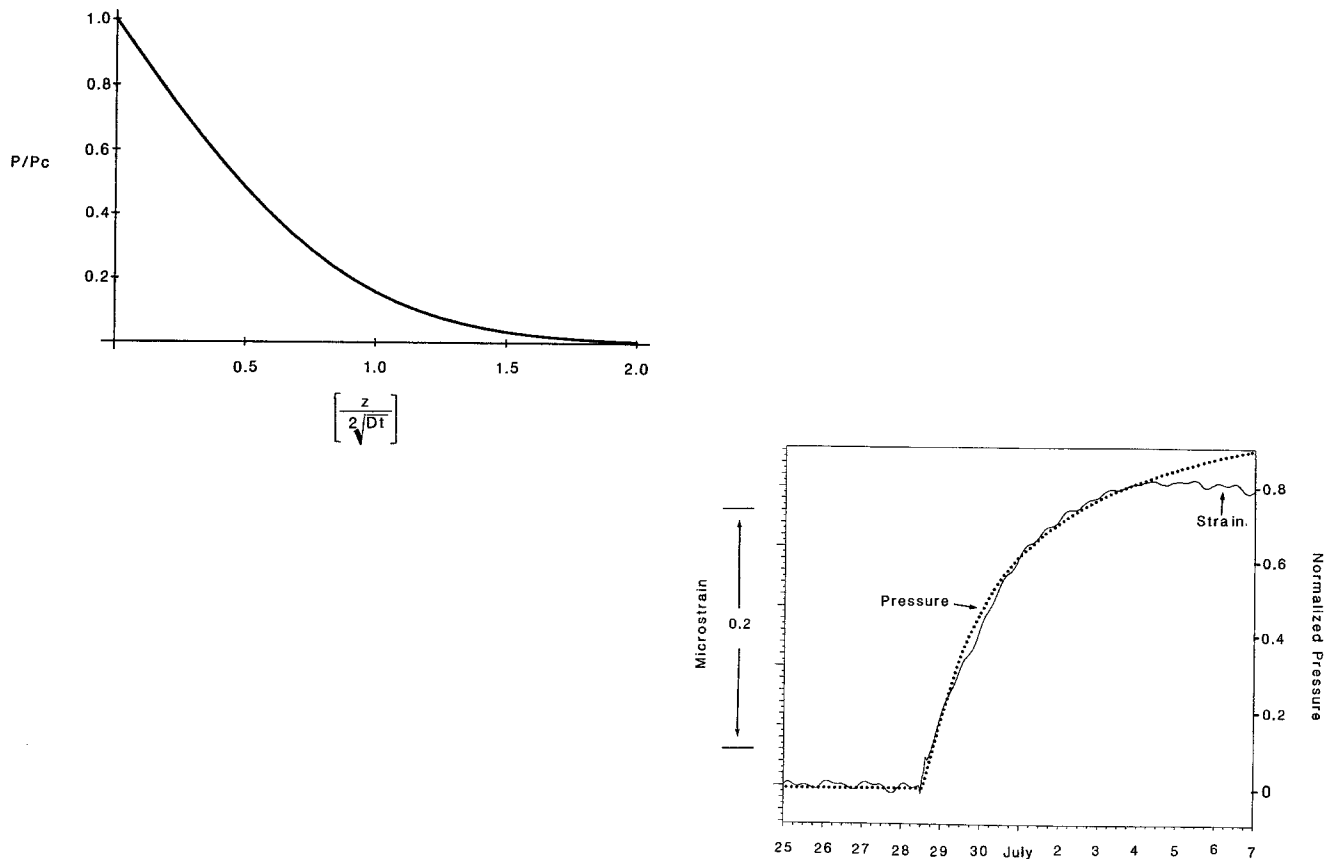


Figure 6. (a) Normalized pore pressure,  $P$ , in a vertical shear fracture as a function of position and time (from Fenoglio *et al.*, 1994). (b) Normalized pore pressure at the end of a 400-m vertical shear fracture as a function of time for parameters used in the text superimposed on the observed strain record from POPA. Atmospheric pressure loading and earth tides have been predicted and removed from the POPA record.

$10^2$  Pa·sec. Leakage from the region would gradually reduce the pressure, and strain resulting from this fluid diffusion from the chamber may be consistent with the observed strain and seismicity decay with time. We note that, if the overpressure zone is within 1.5 source depths of the strainmeter, the sign of the strain change is opposite to that observed. For Mogi-type pressure sources, strains are of the correct sign beyond about 1.5 source depths. To avoid the generation of large displacements within the caldera in violation of the two-color data, the moment of this source can not be more than about  $8 \times 10^{23}$  dyne-cm, or about 40 times the moment of all the triggered seismicity in the caldera.

Thus, for physical mechanisms in the upper crust beneath the caldera, two possibilities remain: (1) either the large amplitude surface waves from the Landers earthquake ruptured isolated compartments in which super-hydrostatic fluid pressure (possibly as high as lithostatic pressure) prevailed and was released to shallower depths, or (2) shaking from the surface waves released gas bubbles within hydrothermal fluid or magma filled regions and produced advective gas overpressure that diffused from the region. Both mechanisms require at least two sources, and both can, with reasonable assumptions about material properties and local

geometry, generate strain, seismicity, and tilt responses similar to those observed. The triggered seismicity shows no coherent migration patterns that might suggest fluid flow. Attempts to identify spatial migration patterns in triggered seismicity under dams have similarly not been productive (Simpson and Negmatullaev, 1981).

Indications of a surge of warm water from greater depth are apparent in disrupted temperature profile records in the 2.3-km-deep well LVEW in the middle of the caldera (Fig. 1) somewhere before 19 July 1992, as shown in Figure 7. Temperature changes are entirely within a cased and cemented section of the borehole and are thus associated with movement of formation water. While the dominant direction of water movement is upward, the dip in the profile between depths of 1700 and 1900 m suggests lateral-to-downward fluid movement locally. This is most likely the result of re-configuration of an interconnected fracture system near the borehole following the Landers earthquake. The transient strain and seismic activity was largely complete by the time these temperature measurements were made (19 July 1992), and we do not have better timing on exactly when this surge of warm water entered the formation near the borehole following the earthquake. An anomalous increase in  $^3\text{He}/^4\text{He}$

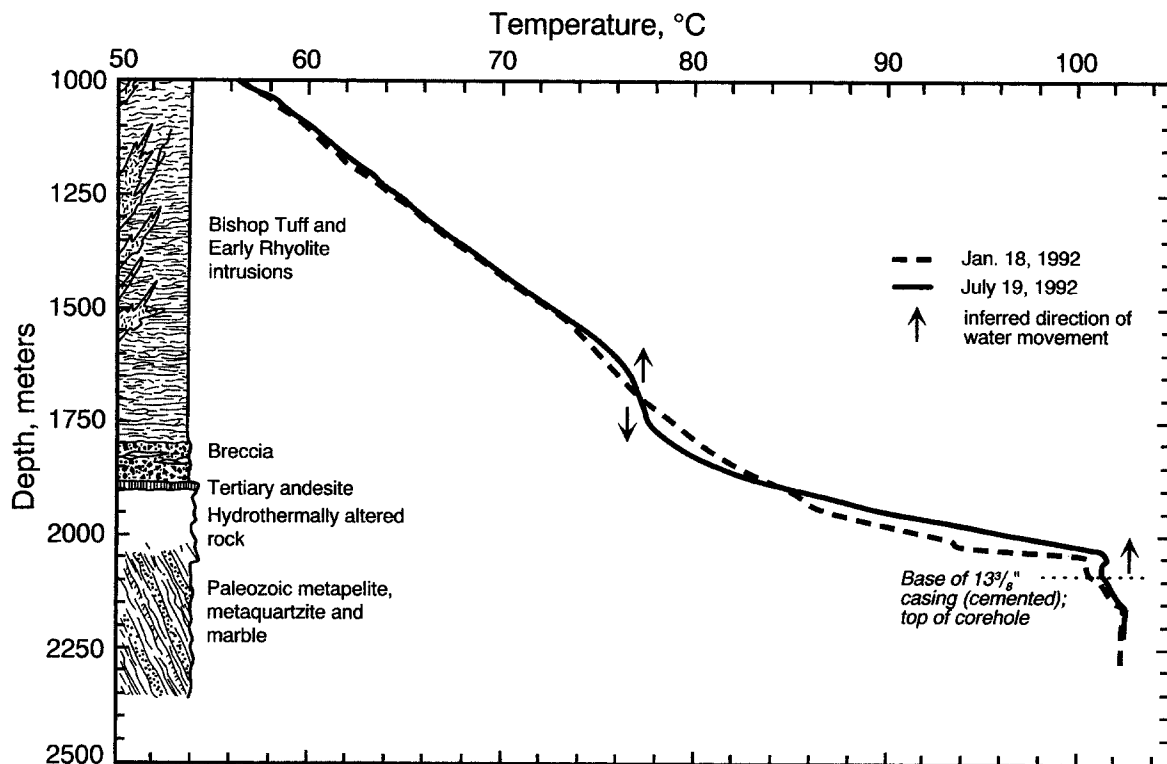


Figure 7. Temperature profiles in the LVEW deep hole before and after the 28 June 1992 Landers earthquake (R. D. Jacobson, personal commun.). Lithology modified from McConnell *et al.* (1992) by Roy A. Bailey.

discharge also occurred on Mammoth mountain at this time (Sorey *et al.*, 1993). Both these observations are consistent with a fluid surge triggered by the Landers earthquake, but neither allow us to identify which is the most likely mechanism.

An argument against the advective overpressure/bubble release mechanism is that similar strain and seismicity effects were not observed during other large distant and local earthquakes. If bubbles are adhering only by surface tension, long-period shaking by the 1989 Loma Prieta earthquake and the 1992 Petrolia earthquake or, perhaps more likely, shorter period shaking from local earthquakes, such as the Chalfant Valley, Eureka Valley, and nearby magnitude 3's and 4's, should have dislodged the bubbles. Threshold triggering of rupture in overpressured chambers would seem an easier way to explain the Landers response and absence of response for other smaller and comparably sized events. A more extensive continuous deformation array, including pore pressure measurements from deep boreholes into the seismogenic zone, would provide a way to separate between the different physical processes in this and other volcanic regions. The primarily distinguishing features would be the different forms of the spatial strain fields expected and the detailed time history of the strains generated.

The observations from Landers clearly show that triggered seismic and deformational activity does occur in remote regions of recent volcanism following large earth-

quakes. It would therefore not be surprising that more extensive volcanic activity, including eruptions, might be triggered in this manner. Possible examples are the eruption of Mt. Fuji in Japan following the 1707  $M = 8.4$  Hoei earthquake (Ishibashi, 1981), the eruption of Mt. Calbuco in Chile (Decker and Decker, 1981) following the 1960  $M = 8.6$  Chilean earthquake, and the Pozzuoli crisis in Italy (Barberi *et al.*, 1984) following the 1980  $M = 6.9$  Iripinia earthquake (Del Pezzo *et al.*, 1983).

### Acknowledgments

We thank John Sass for unpublished temperature data recovered from the deep well in the Long Valley caldera and useful comments from Jim Byerlee and an anonymous reviewer.

### References

- Anderson, J. G., J. N. Brune, J. N. Louie, Y. Zeng, M. Savage, G. Yu, Q. Chen, and D. dePolo (1994). Seismicity in the western Great Basin apparently triggered by the Landers, California, earthquake, 28 June 1992, *Bull. Seism. Soc. Am.* **84**, 863–891.
- Barberi, F., F. Corrado, F. Innocenti, and G. Luongo (1984). Phlegraean Fields 1982–1984: Brief chronicle of a volcano emergency in a densely populated area, *Bull. Volcanol.* **47**, 175–186.
- Beavan, J. (1991). Long baseline tiltmeters: Southern California, in *U.S. Geol. Surv. Open-File Rept. 91-352*, Menlo Park, CA, pp. 225–228.
- Bell, M. L., and A. Nur (1978). Strength changes due to reservoir induced

- pore pressure and stresses and application to Lake Oroville, *J. Geophys. Res.* **83**, 4469–4483.
- Bodin, P. and J. Gomberg (1994). Triggered seismicity and deformation between the Landers, California, and Little Skull Mountain, Nevada, earthquakes, *Bull. Seism. Soc. Am.* **84**, 835–843.
- Byerlee, J. D. (1993). Model for episodic flow of high-pressure water in fault zones before earthquakes, *Geology* **21**, 303–306.
- Davis, P. M. (1986). Surface deformation due to inflation of an arbitrarily oriented triaxial ellipsoidal cavity in an elastic half-space, with reference to Kilauea volcano, Hawaii, *J. Geophys. Res.* **91**, 7429–7438.
- Davis, S. (1993). Remotely triggered microearthquakes at the Geysers geothermal field, California, *EOS* **74**, 317.
- Decker, R. and B. Decker (1981). *Volcanoes*, W. H. Freeman, San Francisco, 244 pp.
- Del Pezzo, E., G. Innaccone, M. Martini, and R. Scarpa (1983). The 23 November 1980 southern Italy earthquake, *Bull. Seism. Soc. Am.* **73**, 173–200.
- du Plessis, J. P. and L. I. Roos (1994). Predicting the hydrodynamic permeability of sandstone with a pore-scale model, *J. Geophys. Res.* **99**, 19771–19776.
- Fenoglio, M. A., M. J. S. Johnston, and J. D. Byerlee (1994). Magnetic and electric fields associated with changes in high pore pressure in fault zones—Application to the Loma Prieta ULF emissions, in *U.S. Geol. Surv. Open-File Rept. 94-228*, pp. 262–278.
- Fournier, R. O. (1985). Continental scientific drilling to investigate brine evolution and fluid circulation in active hydrothermal systems, in *Observation of the Continental Crust through Drilling I*, C. B. Raleigh (Editor), Springer-Verlag, New York, 98–122.
- Fournier, R. O. (1991). The transition from hydrostatic to greater than hydrostatic fluid pressure in presently active hydrothermal systems in crystalline rock, *Geophys. Res. Lett.* **18**, 955–958.
- Fournier, R. O. and R. W. Potter (1982). An equation correlating the solubility of quartz in water from 25 degrees to 900 degrees at pressures up to 10,000 bars, *Cosmochemica Acta* **46**, 1969–1973.
- Gomberg, J. and P. Bodin (1994). Triggering of the  $M_s = 5.4$  Little Skull Mountain, Nevada, earthquake with dynamic strains, *Bull. Seism. Soc. Am.* **84**, 844–853.
- Herrington, R. J. and J. J. Wilkinson (1993). Colloidal Gold and Silica in Mesothermal Vein Systems, *Geology* **21**, 539–542.
- Hill, D. P., P. A. Reasenberg, A. Michael, W. J. Arabaz, G. Beroza, J. N. Brune, D. Brumbaugh, R. Castro, S. Davis, D. dePolo, W. L. Ellsworth, J. Gomberg, S. Harmsen, L. House, S. M. Jackson, M. Johnston, L. Jones, R. Keller, S. Malone, L. Munguia, S. Nava, J. C. Pechmann, A. Sanford, R. W. Simpson, R. S. Smith, M. Stark, M. Stickney, A. Vidal, S. Walter, V. Wong, and J. Zollweg (1993). Seismicity in the Western United States Triggered by the M 7.4 Landers, California, Earthquake of June 28, 1992, *Science* **260**, 1617–1623.
- Hill, D. P., M. J. S. Johnston, J. O. Lanbein, and R. Bilham (1995). Response of Long Valley Caldera to the M = 7.3 Landers, California, earthquake, *J. Geophys. Res.* **100** (in press).
- Ishibashi, K. (1981). Specifications of a soon-to-occur seismic faulting in the Tokai District, Central Japan, based on seismotectonics, *Earthquake Prediction—An International Review*, D. W. Simpson and P. Richards (Editors), American Geophysical Union, Washington, D.C., 297–332.
- Johnston, M. J. S., R. D. Borcherdt, and A. T. Linde (1986). Short-period Strain ( $0.1-10^5$  s): Near source strain for an earthquake ( $M_s 3.2$ ) near San Juan Bautista, California, *J. Geophys. Res.* **91**, 11497–11502.
- Kanamori, H., H.-K. Thio, D. Dreger, and E. Hauksson (1992). Initial investigation of the Landers, California, earthquake of 28 June, 1992, using TERRASCOPE *Geophys. Res. Lett.* **19**, 2267–2270.
- Langbein, J. (1989). Deformation of the Long Valley Caldera, Eastern California from Mid-1983 to Mid-1988: Measurements using a Two-Color Geodimeter, *J. Geophys. Res.* **94**, 3833–3849.
- Langbein, J., D. P. Hill, T. N. Parker, and S. K. Wilkinson (1993). An Episode of Re-inflation of the Long Valley Caldera, Eastern California: 1989–1991. *J. Geophys. Res.* **98**, 15851–15870.
- Linde, A. T., I. S. Sacks, M. J. S. Johnston, D. P. Hill and R. Bilham (1994). Increased pressure from rising bubbles as a mechanism for remotely triggered seismicity, *Nature* **371**, 408–410.
- McConnell, V. S., J. C. Eichelberger, M. J. Keskinen, and P. W. Layer (1992). Geologic Results from the Long Valley Exploratory Well, *Proc. U.S. Dept. Energy Prog. Rev.* **10**, 129–134.
- Mogi, K. (1958). Relations between eruptions of various volcanoes and the deformations of the ground surfaces around them, *Bull. Earthquake Res. Inst., Tokyo Univ.* **36**, 99–134.
- Moore, D. E., D. A. Lockner, and J. D. Byerlee (1994). Reduction of permeability in granite at elevated temperatures, *Science* **265**, 1558–1561.
- Okada, Y. (1992). Internal deformation due to shear and tensile faults in a half-space, *Bull. Seism. Soc. Am.* **82**, 1018–1040.
- Roquemore, G. R. and G. W. Simila (1994). Aftershocks from the 28 June 1992 Landers earthquake: Northern Mojave desert to the Coso volcanic field, California, *Bull. Seism. Soc. Am.* **84**, 854–862.
- Sacks, I. S., S. Suyehiro, D. W. Evertson, and Y. Yamagishi (1971). Sacks-Evertson strainmeter, its installation in Japan and some preliminary results concerning strain steps, *Papers Meteorol. Geophys.* **22**, 195–207.
- Sahagian, D. L. and A. A. Proussevich (1992). Advective bubble overpressure in volcanic systems, *Nature* **359**, 485.
- Silverman, S., Mortensen, C., and M. J. S. Johnston (1989). A satellite-based digital data system for low-frequency geophysical data, *Bull. Seism. Soc. Am.* **79**, 189–198.
- Simpson, D. W. and S. K. Negmatullaev (1981). Induced seismicity at Nurek reservoir, Tadzhikistan, USSR, *Bull. Seism. Soc. Am.* **71**, 1561–1586.
- Sorey, M. L., B. M. Kennedy, C. D. Farrar, and G. A. Suemnicht (1993). Helium isotope and gas discharge variations associated with crustal unrest in Long Valley caldera, California, *J. Geophys. Res.* **98**, 15871–15889.
- U.S. Geological Survey ms977  
Menlo Park, California 94025  
(M.J.S.J., D.P.H., J.L.)
- Carnegie Inst. of Washington  
Dept. Terrestrial Magnetism  
Washington, D.C. 20015  
(A.L.)
- CIRES  
University of Colorado  
Boulder, Colorado 80309-0250  
(R.B.)